Design Constraints for Liquid-Protected Divertors

S. Shin, S. I. Abdel-Khalik†, M. Yoda, and the ARIES Team

G. W. Woodruff School of Mechanical Engineering, Georgia Institute of Technology, Atlanta, GA 30332-0405 USA
[*seungwon.shin@me.gatech.edu*, *said.abdelkhalik@me.gatech.edu, minami.yoda@me.gatech.edu*]

Recent work on liquid-surface-protected plasma facing components has resulted in the establishment of operating windows for candidate liquids, as well as limits on the maximum allowable liquid surface temperature in order to limit plasma impurities from liquid evaporation. In this study, an additional constraint on the maximum allowable surface temperature gradient (i.e., heat flux gradient) has been quantified. Spatial variations in the wall and liquid surface temperatures are expected due to variations in the incident radiation and particle fluxes. Thermocapillary forces created by such temperature gradients can lead to film rupture and dry spot formation in regions of elevated local temperatures. Here, attention has been focused on "non-flowing" thin liquid films similar to those formed on the surface of porous wetted-wall components. Future analyses will include the effects of macroscopic fluid motion, and MHD forces.

A numerical model using the level contour reconstruction method was used to follow the evolution of the liquid free surface above a non-isothermal solid surface. The model was used to develop generalized charts for the maximum allowable spatial temperature gradients (i.e., the critical Marangoni number) as a function of the governing non-dimensional variables, viz. the Weber, Froude, and Prandtl numbers, and aspect ratio. Attention was focused on the asymptotic limit for thin liquid films (i.e., low aspect ratio) which provides a lower bound for the maximum allowable temperature gradients. Specific examples for lithium, Flibe, lithium-lead, tin, and gallium are presented. The generalized charts developed in this investigation will allow reactor designers to identify design windows for successful operation of liquid-protected plasma facing components for various coolants, film thicknesses, and operating conditions.

I. INTRODUCTION

Work on liquid-surface-protected plasma facing components, and plasma surface interactions, has been performed by the Advanced Power Extraction (APEX) study and the Advanced Limiter-Divertor Plasma Facing Systems (ALPS) Program [1, 2]. The attractiveness of this concept derives from the ability of the liquid to remove the incident heat load, while protecting the underlying solid wall from radiation damage, erosion, and thermal stress. A detailed reactor design study with liquid first wall and divertor has recently been reported by the APEX team [3]; both liquid metals and molten salts have been investigated. State-of-the-art codes have been used to model the plasma edge, plasma sheath at the divertor, and particle surface interactions to establish the operating windows for candidate liquids [4]. Lithium, Flibe, lithium-lead, lithium-tin, tin, and gallium were among the liquids examined. Plasma impurity levels resulting from liquid evaporation impose maximum surface temperature limits ranging from 380ºC for Li to 1630ºC for Sn [3, 4].

This study is aimed at quantifying the limits, if any, on the maximum allowable temperature gradient to assure liquid film stability on liquid-surface-protected plasma facing components. Spatial variations in the wall and liquid surface temperatures are expected in all magnetic fusion devices due to variations in the incident radiation and particle flux. Such spatial variations in temperature induce the so-called "thermocapillary" effect, which derives from the surface tension gradient along a two-phase interface. For most liquids, surface tension decreases with temperature. Thermocapillary forces can hence lead to film rupture and dry spot formation in regions of elevated temperatures. While this phenomenon has been extensively examined by the fluid mechanics community, it has not, to our knowledge, been considered by the fusion community in analyzing the feasibility of liquid protected plasma facing components. Here, our attention will be focused on "non-flowing" thin liquid films similar to those formed on the surface of porous wetted-wall components. Future analyses will include the effects of macroscopic fluid motion, and MHD forces.

Several studies dealing with this non-linear free-boundary problem have been reported in the literature [5-11]. Ruckenstein and Jain used long-wave theory to study the instability of an ultra thin liquid film on a solid surface [5]. A small perturbation was imposed on the liquid-gas interface; the growth of the perturbation in time was investigated using linear theory. The Navier-Stokes equation was used to describe the interface motion by including a body force term to account for London/van der Waals interaction. Atherton and Homsy derived the nonlinear partial differential (evolution) equations describing the movement of a fluid-fluid interface for long interfacial waves in two-phase flow, including a detailed treatment of interfacial boundary conditions in both Euclidean and non-Euclidean coordinates [6]. Davis examined nonlinear effects in thin film instability [7], and formulated a strongly nonlinear evolution equation for the

thickness of a static film on a planar solid including London/van der Waals forces. He later extended his theory to include variable surface tension in deriving a long-wave evolution equation for the interface shape subject to an external temperature gradient with arbitrary orientation for the purpose of studying thermocapillary instability [8].

Tan, *et al.* imposed a non-uniform spatially periodic temperature distribution along the underlying plate, and examined the response of the liquid layer to thermocapillary effects [9]. The system is subject to gravity, which induces hydrostatic effects; both London/van der Waals and surface tension forces have been included. They developed a nonlinear long-wave equation for the shape of the thin film, and found that a continuous steady liquid layer could be sustained only if the temperature gradient at the underlying solid surface was less than a critical value. Burelbach, *et al.* [10] validated the theoretical formulation of Tan, *et al* in a carefully designed experiment for thin films. Ref. 11 reviews previous work on long scale evolution of thin films. More recently, direct numerical simulation of the evolution of free liquid surfaces has been performed using the level contour reconstruction method [12, 13], which stems from Tryggvason's finite difference/front tracking method originally developed for two- and three-dimensional isothermal multi-fluid flows [14, 15].

The remainder of this paper is organized as follows. Section II includes the formulation of the governing equations for thrmocapillary flows of a thin liquid layer on a non-isothermal solid wall; the governing equation for the shape of the liquid film for low aspect ratios (i.e. thin films), hereafter referred to as the "asymptotic solution," is first presented. The results, including generalized non-dimensional charts for the maximum allowable temperature gradient as a function of the governing non-dimensional parameters, along with specific results for various liquid candidates, are presented in Section III. Conclusions are given in Section IV.

II. THEORETICAL MODEL

II.1. Asymptotic Solution

Consider the system shown in Figure 1. Here, a thin liquid film with an initially uniform thickness h_o rests atop a solid surface with a non-uniform, spatially-periodic, temperature distribution (period L). Variations in the z-direction (*viz*. toroidal direction) are ignored, so that the problem becomes two-dimensional. Following the method of Tan, *et al.* [9], for low aspect ratios, the long-wave equation for the non-dimensional steady-state shape of the thin liquid film (the Asymptotic Solution) is given by:

$$\frac{a^2\mathrm{Fr}}{\mathrm{We}}\frac{\partial^3 h'}{\partial x'^3}h' + \frac{\partial h'}{\partial x'}h' + \frac{3}{2}(\mathrm{M}/\mathrm{Pr})\cdot\mathrm{Fr}\frac{\partial T_s'}{\partial x'} = 0 \qquad (1)$$

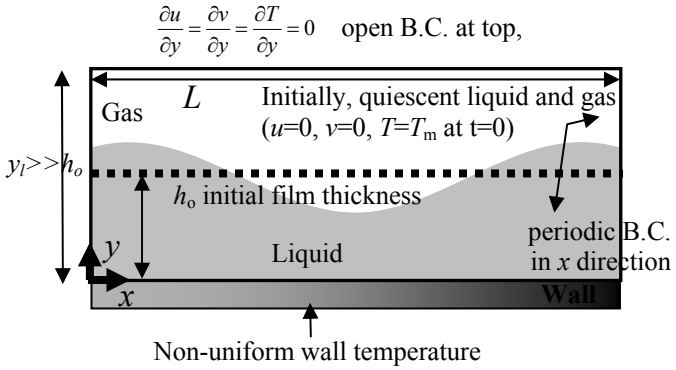

Fig. 1. Initial surface configuration and boundary conditions used to model horizontal surface subjected to temperature gradient.

Here,

$$a=\frac{h_o}{L};\ h'=\frac{h}{h_o};\ x'=\frac{x}{L}=\frac{ax}{h_o};\ \mathrm{Fr}=\frac{V_g^2}{gh_o}=\frac{\mu_L^2}{g\rho_L^2h_o^3};$$

$$\mathrm{We}=\frac{\mu_L^2}{\rho_L\sigma_o h_o};\ \mathrm{Pr}=\frac{\mu_L c_L}{k_L};\ \mathrm{M}=\frac{\gamma_o\Delta T_s h_o}{\mu_L\alpha_L};$$

$$T'=\frac{T-T_m}{\Delta T_s};\ \text{and}\ V_g=\frac{\mu_L}{\rho_L h_o}$$

are the aspect ratio, non-dimensional film thickness, normalized x-coordinate, Froude, Weber, Prandtl, and Marangoni numbers, normalized temperature, and scaling velocity. The quantity γ_o is the absolute value for the rate of change of surface tension with temperature.

Following the procedure described by Tan, *et al.* [9], equation (1) can be solved by approximating the solution for h' by an N-term truncated Fourier cosine series; the coefficients of the expansion of h' are determined using Galerkin's method. With a, Fr, and We as independent parameters, equation (1) is repeatedly solved for a given wall temperature distribution to determine the critical temperature gradient, *i.e.*, the (aM/Pr) value corresponding to zero film thickness (h'=0) at the point of maximum wall temperature (center of the wall; x= L/2).

II.2. Numerical Solution

Full direct numerical simulation has also been performed using the level contour reconstruction method [12, 13]. The method has been simplified by eliminating logical connectivity, and thus eliminating the associated algorithmic burden, while retaining the accuracy and advantages of explicit Lagrangian surface tracking.

The non-dimensional governing equations for mass and momentum conservation are given by:

$$\frac{\partial u'}{\partial x'}+\frac{\partial v'}{\partial y'}=0 \qquad (2)$$

$$a^2\rho^+\left[\frac{\partial u'}{\partial t'}+u'\frac{\partial u'}{\partial x'}+v'\frac{\partial u'}{\partial y'}\right]$$
$$=-\frac{\partial p'}{\partial x'}+a^2\frac{\partial}{\partial x'}\left(2\mu^+\frac{\partial u'}{\partial x'}\right)+\frac{\partial}{\partial y'}\left(\mu^+\frac{\partial u'}{\partial y'}\right)$$
$$+a^2\frac{\partial}{\partial y'}\left(\mu^+\frac{\partial v'}{\partial x'}\right)+\int\left(\sigma'\kappa\mathbf{n}+\frac{\partial\sigma'}{\partial s}\mathbf{t}\right)\delta ds\cdot\hat{\mathbf{i}} \qquad (3)$$

$$a^4\rho^+\left[\frac{\partial v'}{\partial t'}+u'\frac{\partial v'}{\partial x'}+v'\frac{\partial v'}{\partial y'}\right]$$
$$=-\frac{\partial p'}{\partial y'}+\frac{\rho^+}{\mathrm{Fr}}+a^4\frac{\partial}{\partial x'}\left(\mu^+\frac{\partial v'}{\partial x'}\right)+a^2\frac{\partial}{\partial x'}\left(\mu^+\frac{\partial u'}{\partial y'}\right)$$
$$+a^2\frac{\partial}{\partial y'}\left(2\mu^+\frac{\partial v'}{\partial y'}\right)+a\int\left(\sigma'\kappa\mathbf{n}+\frac{\partial\sigma'}{\partial s}\mathbf{t}\right)\delta ds\cdot\hat{\mathbf{j}} \qquad (4)$$

Here p' is the pressure and κ is twice the mean interface curvature. We assume that the surface tension at the liquid-gas interface σ varies linearly with the temperature T from the reference value at T_m; the non-dimensional surface tension coefficient, σ', can then be expressed by:

$$\sigma'=1/\mathrm{We}-(\mathrm{M/Pr})T' \qquad (5)$$

Neglecting evaporation at the liquid-gas interface, the energy equation becomes:

$$a^2\rho^+\left[\frac{\partial c^+T'}{\partial t'}+u'\frac{\partial c^+T'}{\partial x'}+v'\frac{\partial c^+T'}{\partial y'}\right]$$
$$=\frac{a^2}{\mathrm{Pr}}\frac{\partial}{\partial x'}\left(k^+\frac{\partial T'}{\partial x'}\right)+\frac{1}{\mathrm{Pr}}\frac{\partial}{\partial y'}\left(k^+\frac{\partial T'}{\partial y'}\right) \qquad (6)$$

One set of transport equations (2), (3), (4), and (6), valid for both fluids, is solved. This local single-field formulation incorporates the effect of the interface in the equations as delta-function source terms which act only at the interface and automatically satisfy the interface boundary conditions. The delta-function source term in equations (3) and (4) represents the surface tension force exerted on a differential element at the interface (Fig. 2):

$$\delta F_e=\int_{\Delta s}\left[\sigma\kappa\mathbf{n}+\frac{\partial\sigma}{\partial s}\mathbf{t}\right]ds=\int_B^A\frac{\partial(\sigma\mathbf{t})}{\partial s}ds$$
$$=(\sigma_A\mathbf{t}_A-\sigma_B\mathbf{t}_B) \qquad (7)$$

where

$$\sigma\kappa\mathbf{n}+\frac{\partial\sigma}{\partial s}\mathbf{t}=\sigma\frac{\partial\mathbf{t}}{\partial s}+\frac{\partial\sigma}{\partial s}\mathbf{t}=\frac{\partial(\sigma\mathbf{t})}{\partial s} \qquad (8)$$

The first and second term in equation (8) represent the normal surface tension force and the thermocapillary force, respectively. A more detailed description of the Level Contour Reconstruction techniques and procedures can be found in Refs. 12 and 13.

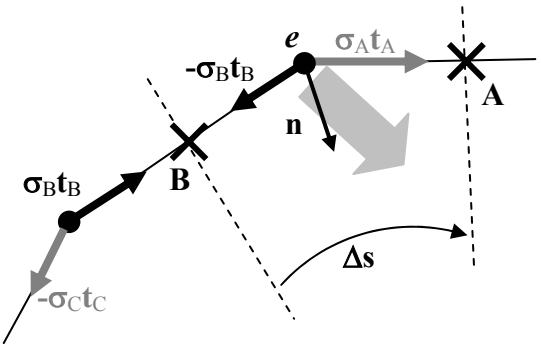

Fig. 2. Schematic diagram of the surface tension force formulation. (**n** : unit vector in normal direction. **t** : unit vector in tangential direction)

III. RESULTS

III.1. Asymptotic Solution

The results of the asymptotic solution can be presented as generalized charts for the maximum non-dimensional temperature gradient (*i.e.*, critical value for aM/Pr) as a function of the Weber and Froude numbers (Fig. 3) with a given aspect ratio (a=0.02) and a prescribed sinusoidal wall temperature distribution:

$$T_s'(x')=\cos\left[2\pi(x'-0.5)\right] \qquad (9)$$

The maximum non-dimensional temperature gradient (aM/Pr) is defined by:

$$a\mathrm{M/Pr}=\frac{(\Delta T_s/L)}{(\mu_L^2/\rho_L\gamma_o h_o^2)} \qquad (10)$$

Referring to Figure 3, for small values of (1/Fr), the maximum temperature gradient is proportional to (1/We), while at high (1/Fr) values, it is independent of the Weber number. Plots similar to those shown in Figure 3 have been obtained for other aspect ratios. It can be shown that in the limit of zero aspect ratio, $(a\mathrm{M/Pr})_{cr}$ approaches a value of $(\pi^2 a/12\mathrm{Fr})$, independent of the Weber number.

III.2. Numerical Solution

For high aspect ratios, the level contour reconstruction method described in Section II.2 above has been used to solve the full set of conservation equations. Generalized charts for the maximum non-dimensional temperature gradients as a function of the Weber, Froude, and Prandtl numbers, and aspect ratio have been obtained. The simulation geometry is the same as that used to develop the asymptotic solution (Fig. 1). The liquid interface is assumed to be initially flat, while both the liquid and gas are assumed to be initially quiescent (u,v=0 and T=T_m at t=0). A non-uniform temperature distribution is imposed on the bottom wall (Eq. 9). The evolution of

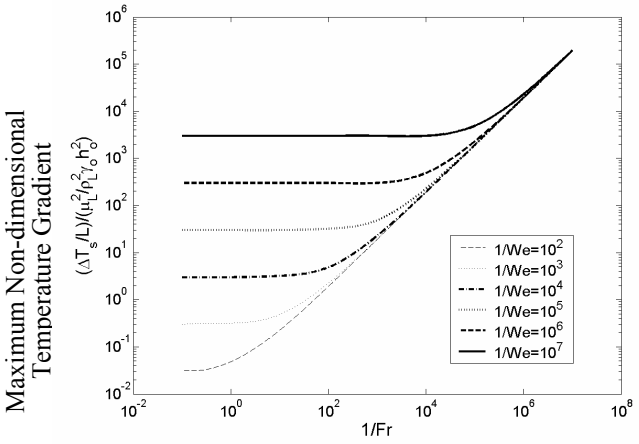

Fig. 3. Generalized non-dimensional charts for the maximum nondimensional temperature gradient from asymptotic solution

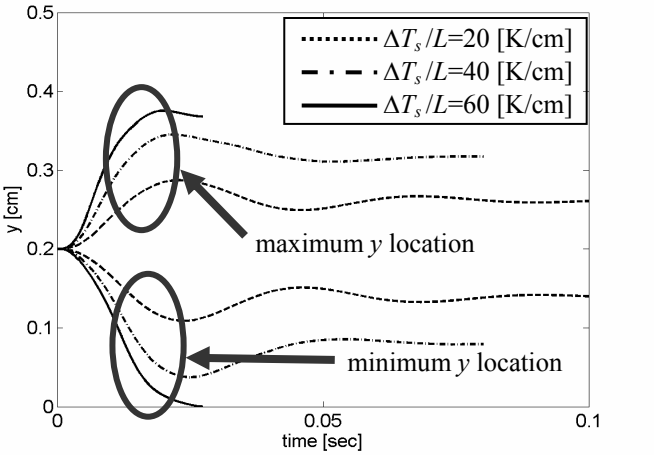

Fig. 4. Transient profile of the maximum and minimum interface point by 2D simulation of full equation using the Level Contour Reconstruction Method

the free surface is then followed until steady state conditions are reached. Typical results for a lithium film with three different temperature gradients (20, 40, and 60 K/cm) are shown in Figure 4. These two-dimensional simulations were performed using a 250×50 mesh resolution with a 1[cm]×0.1[cm] box size, and an initial film thickness of 0.2 mm. For each case, the transient evolutions of the maximum and minimum film thickness along the surface are depicted; as the temperature gradient increases, the minimum thickness reaches zero indicating film rupture.

A typical generalized non-dimensional chart for the maximum non-dimensional temperature gradient as a function of the Weber and Prandtl numbers is shown in Figure 5. These results correspond to a (1/Fr) value of 10^3 and an aspect ratio of 0.02. The corresponding values predicted by the asymptotic solution are also shown. Similar charts for other values of (1/Fr) and aspect ratios have been obtained. These results indicate that the maximum allowable non-dimensional temperature gradient increases with Pr and that the asymptotic solution represents the case of zero Prandtl number (i.e. the conduction limit), and can, therefore, be viewed as a conservative lower bound.

III.3. Application to Candidate Liquids

Both the asymptotic solution and the full numerical simulation have been used to determine the maximum allowable temperature gradients for various candidate coolants, namely, lithium, lithium-lead, Flibe, tin, and gallium. Table I lists values of the non-dimensional parameters for the five fluids at different temperatures with a nominal film thickness of 1.0 mm. The corresponding maximum temperature gradients predicted by both the asymptotic solution and the numerical simulation are shown in Table II. These results show that the allowable temperature gradients differ significantly among the candidate fluids, and that, in some cases, such constraint may be highly restrictive.

IV. CONCLUDING REMARKS

In this study, limits on the maximum allowable wall surface temperature gradients (*i.e.*, spatial heat flux gradients) in liquid-surface-protected plasma facing components have been quantified. Operation beyond these limits may lead to film rupture and dry spot formation in regions of elevated temperatures due to

Table I. Values of the nondimensional variables for different Coolants with nominal thickness of 1 mm

Parameter	Lithium		Lithium-Lead		Flibe		Tin		Gallium	
	573K	773K	573K	773K	573K	773K	1073K	1473K	873K	1273K
Pr	0.042	0.026	0.031	0.031	0.013	2.4	0.0047	0.0035	0.0058	0.0029
1/Fr	1.2×10^4	2.2×10^5	1.9×10^5	6.3×10^5	1.2×10^3	3.8×10^4	5.3×10^5	6.7×10^5	5.7×10^5	8.2×10^5
1/We	7.8×10^5	1.3×10^6	9.4×10^5	3.0×10^6	1.3×10^4	4.0×10^5	4.2×10^6	4.8×10^6	6.9×10^6	1.0×10^7
$\mu_L^2/(\rho_L\gamma_o h_o^2)$[K/m]	2.8	1.5	4.4	1.3	140	4.3	0.72	0.55	1.6	1.1

Coolant	Mean Temperature [K]	$(\Delta T_s/L)$ [K/cm]	
		Numerical Solution	Asymptotic Solution
Lithium	573	30	13
Lithium -Lead	673	570	173
Flibe	673	76	38
Tin	1273	113	80
Gallium	1073	600	211

Table II. The maximum temperature gradient limit for different coolants

thermocapillary forces. Generalized charts have been developed to allow designers of fusion systems to identify design windows for successful operation of liquid-protected plasma facing components. An asymptotic solution which provides a conservative lower bound on the allowable temperature gradient has been developed. Detailed numerical simulations have also been used to obtain more accurate limits for cases with high aspect ratios. The results have been applied to five different candidate fluids, namely, lithium, lithium-lead, flibe, tin, and gallium. These results show that the maximum allowable temperature gradients differ by more than an order of magnitude, with lithium having the lowest allowable temperature gradient and gallium the highest.

ACKNOWLEDGMENTS

This work has been performed as a part of the ARIES-CS Study. We gratefully acknowledge the financial support provided by the U.S. Department of Energy Office of Fusion Energy Sciences through contract number DE-FG02-01ER54656.

REFERENCES

[1] M. A. ABDOU, and APEX TEAM, "Exploring Novel High Power Components for Attractive Fusion Systems," *Fusion Eng. Design* **45**, 145 (1999). [http://www.fusion.ucla.edu/APEX/]

[2] R. MATTAS, and ALPS TEAM, "ALPS - Advanced Limiter-Divertor Plasma Facing Systems," *Fusion Eng. Design*, **49-50**, 127 (2000). [http://fusion.anl.gov/ALPS_Info_Center/calls.html]

[3] R. E. NYGREN, ET AL., "A Fusion Reactor Design with a Liquid First Wall and Divertor," to appear in *Fusion Eng. Design*, (2004).

[4] T. D. ROGNLIEN and M. E. RENSINK, "Interaction between Liquid-Wall Vapor and Edge Plasmas," *J. Nucl. Materials*, **290-293**, 312 (2001).

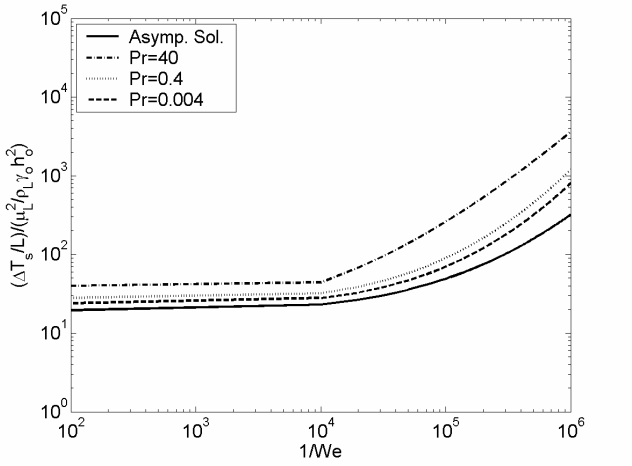

Fig. 5. Generalized non-dimensional charts for the maximum nondimensional temperature gradient from full numerical simulation with $1/Fr=10^3$

[5] E. RUCKENSTEIN and R. K. JAIN, "Spontaneous rupture of Thin Liquid Film," *J. Chem. Soc. Farad. T. 2*, **70**, 132 (1974).

[6] R. W. ATHERTON and G. M. HOMSY, "On the Derivation of Evolution Equation for Interfacial Waves," *Chem. Eng. Commun.*, **2**, 57 (1976).

[7] S. H. DAVIS, "Rupture of Thin Liquid Films," *Waves on Fluid Interfaces*, 291, R. E. Meyer, Ed., Academic Press, New York (1983).

[8] S. H. DAVIS, "Thermocapillary Instability," *Annu. Rev. Fluid Mech.*, **19**, 403 (1987).

[9] M. J. TAN, S. G. BANKOFF, and S. H. DAVIS, "Steady Thermocapillary Flows of Thin Liquid Layers: I. Theory," *Phys. Fluids A*, **2**, 313 (1990).

[10] J. P. BURELBACH, S. G. BANKOFF, and S. H. DAVIS, "Steady Thermocapillary Flows of Thin Liquid Layers: II. Experiment," *Phys. Fluids A*, **2**, 322 (1990).

[11] A. ORON, S. H. DAVIS, and S. G. BANKOFF, "Long-Scale Evolution of Thin Liquid Films," *Reviews of Modern Physics*, **69**, 931 (1997).

[12] S. SHIN, "A Level Contour Reconstruction Method for Three-Dimensional Multiphase Flows and Its Application," *Ph.D. Thesis*, Georgia Institute of Technology (2002).

[13] S. SHIN and D. JURIC, "Modeling Three-Dimensional Multiphase Flow Using a Level Contour Reconstruction Method for Front Tracking Without Connectivity," *J. Comput. Phys.*, **180**, 427 (2003).

[14] S. O. UNVERDI and G. TRYGGVASON, "A Front-Tracking Method for Viscous Incompressible Multi-Fluid Flows," *J. Comput. Phys.*, **100**, 25 (1992).

[15] S. O. UNVERDI and G. TRYGGVASON, "Computations of Multi-Fluid Flows," *Physica D*, **60**, 70 (1992).